Journal of Photonics for Energy

PhotonicsforEnergy.SPIEDigitalLibrary.org

Chlorin e6 sensitized photovoltaic cells: effect of co-adsorbents on cell performance, charge transfer resistance, and charge recombination dynamics

Sherard K. S. Lightbourne
Habtom B. Gobeze
Navaneetha K. Subbaiyan
Francis D'Souza

SPIE.

Chlorin e6 sensitized photovoltaic cells: effect of co-adsorbents on cell performance, charge transfer resistance, and charge recombination dynamics

Sherard K. S. Lightbourne, Habtom B. Gobeze, Navaneetha K. Subbaiyan,[†] and Francis D'Souza*
University of North Texas, Department of Chemistry, 1155 Union Circle, #305070, Denton, Texas 76203-5017, United States

Abstract. The effect of dye-aggregation-preventing co-adsorbents, cholic acid and deoxycholic acid, on the performance of dye-sensitized solar cells constructed using a metal-free sensitizer, chlorin e6 adsorbed onto TiO_2 surface is investigated. Absorption and fluorescence studies of chlorin e6 provided the spectral coverage, whereas electrochemical studies allowed estimation of the free energy of charge injection. B3LYP/6-31G* studies were performed to visualize location of the Frontier orbitals and their contribution to the charge injection when they were surface-modified on TiO_2. The concentration of the co-adsorbent and soaking time was optimized for improved cell performance. Better dye regeneration efficiency for co-adsorbed cells compared to the cells with no co-adsorbent was revealed by electrochemical impedance spectroscopy. Femtosecond transient absorption studies were performed to probe the kinetics of charge injection and charge recombination on the TiO_2/chlorin e6/co-adsorbent electrodes. Such studies showed slower by an order of magnitude charge recombination rates for electrodes co-adsorbed either with cholic acid or deoxycholic acid while maintaining almost the same charge injection rates, thus rationalizing the importance of co-adsorbents on the overall cell performance. [DOI: 10.1117/1.JPE.5.053089]

Keywords: photoelectrochemistry; chlorin e6; impedance spectroscopy; light energy conversion; femtosecond transient spectroscopy; charge recombination dynamics.

Paper 15032 received Mar. 21, 2015; accepted for publication Jun. 17, 2015; published online Jul. 13, 2015.

1 Introduction

Dye sensitized solar cells (DSSCs) have been recognized as one of the promising light energy harvesting technologies,[1,2] and using porphyrin as sensitizers, light-to-electricity conversion efficiency (η) of 12.3% has been accomplished.[3–6] This improvement has been attributed to several factors including molecular engineering of the sensitizers to match the useful portion of the solar spectrum,[3] and ways to control the arrangement of dye molecules at the semiconductor/dye interface to ease the process of reverse charge transfer and exciton annihilation.[7,8]

Traditionally luminescent metal complexes[9,10] and porphyrins[4–6,11–13] have been used to fulfill the role of sensitizers. However, compounds derived from naturally occurring chlorophylls are appealing as they are abundant, inexpensive in nature, and are feasible for molecular structure modification methods.[14–17] A large number of studies have focused on chlorin e6 due to its ease of synthesis from the precursor molecule, chlorophyll *a*.[18–22] In the construction of solar cells, co-adsorbents were used to minimize the strong aggregation effects caused by chlorin e6. Improved performance was often achieved using this approach, but the photochemical reasons for this performance were not reported.[20] In the present study, we have built DSSCs

*Address all correspondence to: Francis D'Souza, E-mail: Francis.DSouza@unt.edu

[†]Present address: Center for Integrated Nanotechnologies, Chemistry Division, Los Alamos National Laboratory, Los Alamos, New Mexico 87544, United States.

1947-7988/2015/$25.00

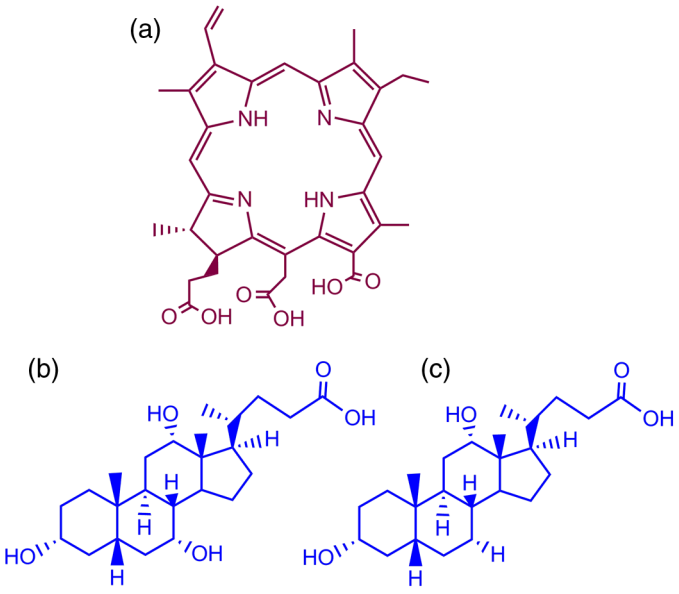

Fig. 1 Structures of the sensitizer, (a) chlorin e6, and co-adsorbents, (b) cholic acid, and (c) deoxycholic acid used in the present study.

using chlorin e6 adsorbed onto TiO_2 surface in the presence of co-adsorbents, cholic acid and deoxycholic acid (see Fig. 1 for the structures of the sensitizer and co-adsorbents). The effect of the co-adsorbents on the dye regeneration efficiency, and charge injection and recombination dynamics is systematically investigated using electrochemical impedance spectroscopy (EIS) and femtosecond transient absorption techniques, respectively.

2 Experimental Methods

2.1 *Chemicals*

Chlorin e6 was procured from Frontier Chemicals (Logan, Utah) and used as received. All of the reagents and chemicals were from Aldrich Chemicals (Milwaukee, Wisconsin) and Solaronix SA.

2.2 *Spectral Measurements*

The UV–visible measurements were carried out either using a Jasco V-670 spectrophotometer or a Shimadzu Model 2550 double monochromator UV–visible spectrophotometer. The steady-state fluorescence spectra were measured using a Horiba Jobin Yvon Nanolog UV–visible–NIR spectrofluorometer equipped with a photomultiplier tube (for UV–visible) and InGaAs (for NIR) detectors. Cyclic voltammograms were recorded on an EG&G 263A potentiostat/galvanostat using a three-electrode system. A platinum button electrode was used as the working electrode, whereas a platinum wire served as the counter electrode and an Ag/AgCl electrode was used as the reference electrode. Ferrocene/ferrocenium redox couple was used as an internal standard. All the solutions were purged prior to electrochemical and spectral measurements with nitrogen gas. The fluorescence lifetimes were measured with the time-correlated single-photon counting (TCSPC) lifetime option with nano-LED excitation sources on the Nanolog.

2.3 *Photoelectrochemical Measurements*

Photoelectrochemical measurements were performed using the Grätzel-type two-electrode system using fluorine-doped tin oxide (FTO) (~10 to 12 μm, tec7 grade from Pilkington) glass coated with thin-film TiO_2 as the working electrode and platinized FTO as the counter electrode.

The thin-film TiO_2 was prepared via the "Doctor-Blade" technique. A mediator electrolyte solution containing 0.1 M LiI, 0.05 M I_2, 0.5 M 4-tert-butylpyridine, and 0.6 M 1-methyl-3-propylimidazolium iodide in acetonitrile was injected between the electrodes.

The photocurrent–photovoltage characteristics were collected using a Keithley Instruments Inc. (Cleveland, Ohio) Model 2400 current/voltage source meter under illumination from a simulated light source using a Model 9600 of 150-W Solar Simulator of Newport Corp. (Irvine, California) and filtered using an AM 1.5 filter. Incident photon-to-current efficiency (IPCE) measurements were performed under ~4 mW cm^2 monochromatic light illumination conditions using a setup comprised of a 150 W Xe lamp with a Cornerstone 260 monochromator (Newport Corp., Irvine, California).

2.4 *Electrochemical Impedance Measurements*

Electrochemical impedance measurements were performed using an EG&G PARSTAT 2273 potentiostat/galvanostat. Impedance data were recorded under forward-bias condition from 100 kHz to 50 mHz with an AC amplitude of 10 mV. Data were recorded under dark and AM 1.5 illumination conditions applying corresponding open-circuit potential (V_{oc}). The data were analyzed using ZSimpwin software from Princeton Applied Research. Solution resistance (R_s), charge transfer resistance (R_{ct}), and capacitance due to constant phase element (Q) were deduced from the fitted data. Constant phase element was considered as a capacitance component of the double-layer electrode interface due to the roughness of the electrode.

The computational calculations were performed by DFT B3LYP/6-31G* methods with Gaussian 09 software package[23] on high-speed computers. The HOMO and LUMO orbitals were generated using the GuessView program.

2.5 *Femtosecond Transient Absorption Spectral Measurements*

Femtosecond transient absorption spectroscopy experiments were performed using an ultrafast femtosecond laser source (Libra) by Coherent incorporating a diode-pumped, mode-locked Ti: sapphire laser (Vitesse), and diode-pumped intra cavity doubled Nd:YLF laser (Evolution) to generate a compressed laser output of 1.45 W. For optical detection, a Helios transient absorption spectrometer coupled with femtosecond harmonics generator both provided by Ultrafast Systems was used. The source for the pump and probe pulses was derived from the fundamental output of Libra (compressed output 1.45 W, pulse width 91 fs) at a repetition rate of 1 kHz. Ninety-five percent of the fundamental output of the laser was introduced into harmonic generator which produces second and third harmonics of 400 and 267 nm besides the fundamental 800 nm for excitation, whereas the rest of the output was used for generation of white light continuum. In the present study, the second harmonic 400-nm excitation pump was used in all the experiments. Kinetic traces at appropriate wavelengths were assembled from the time-resolved spectral data. All measurements were conducted at 298 K.

2.6 *Preparation of Electrodes for Photoelectrochemical and Transient Studies*

Electrodes were prepared by first cleaning FTO using soap and deionized water, then by sonicating individually in solutions of 0.1 M HCl, acetone, and isopropanol for 10 min each. Next, the FTO was placed on a hotplate at 200°C for 15 min and cooled to 80°C for 15 min. Once cooled to 80°C, FTO was allowed to soak in preheated (30 min, 70°C) 40 mM solution of $TiCl_4$ for 30 min at 70°C. After soaking, FTO was rinsed in Millipore water and methanol. Next, FTO was heated for 15 min at 445°C and cooled to 80°C. Then, a layer of 15 to 20 nm anatase TiO_2 (Ti-Nanoxide T/SP, Solaronix) was applied on the surface of the FTO using the doctor blade technique and allowed to dry in air for 20 min. The FTO/TiO_2 was then annealed in a heat cycle of 130, 230, 330, 395, 440, and 515°C for 10 min each. After cooling, a second layer of 15 to 20 nm anatase TiO_2 was applied and annealed in a similar fashion. Following the second annealing phase, FTO was allowed to cool at 80°C for 15 min and then cut into six separate but equal parts. Next, the electrodes were allowed to soak in a fresh preheated (30 min, 70°C) $TiCl_4$ solution for an additional 30 min at 70°C. After the electrodes had been soaked in $TiCl_4$

solution, they were rinsed in Millipore water and methanol. The films were then annealed at 445°C for 15 min and then cooled at 80°C for 15 min before immersing in a 0.3 mM sensitizer solution for a specified duration of time.

2.7 *Preparation of Platinized Electrodes*

FTO glass electrodes were washed as aforementioned. After washing, each strip of FTO was heated at 440°C for 15 min and then cooled at 80°C for another 15 min. Each strip was then cut into six smaller electrodes of similar size and dusted with N_2 before applying a solution containing 1 mg of chloroplatinic acid in 2 mL of ethanol. The electrodes were then heated at 440°C a second time for 15 min before allowing them to cool at 80°C for 15 min.

3 Results and Discussion

3.1 *Optical Absorbance, Fluorescence, Electrochemical, and Computational Studies*

Figure 2 shows the optical absorbance and fluorescence spectra of chlorin e6 in methanol. In agreement with the previous reports,[18,19] an intense Soret band at 400 nm and visible bands at 500, 530, 555, 605 and 660 nm were observed. That is, spectral coverage from 300 to 700 nm for this sensitizer was noted. Chlorin e6 also revealed a fluorescence peak at 667 nm. Lifetime of this probe was determined from TCSPC method using a 494 nm nano-LED excitation source. The time profile could be fitted to a monoexponential decay ($\chi^2 = 1.19$) that resulted in a lifetime of 4.73 ns.

Further, cyclic voltammograms of chlorin e6 in dimethylformamide (DMF) containing 0.1 M $(TBA)ClO_4$ was recorded as shown in Fig. 3(a). An irreversible oxidation at 0.76 V versus Ag/AgCl was observed. There was a prewave at 0.57 V during the first cycle which disappeared during the second cycle, perhaps due to some adsorbed species on the electrode surface. Differential pulse voltammetry provided peak potential value of 0.72 V versus Ag/AgCl for the first oxidation of chlorin e6. Two quasireversible reductions with peak potentials located at −1.06 and −1.28 were also observed. The oxidation process of chlorin e6 was found to be lower than that of free-base tetraphenylporphyrin, commonly used in building DSSCs.[23] Furthermore, the excited state reduction potential and free-energy change for electron injection were calculated according to Rehm–Weller approximation,[24] using Eqs. (1) and (2), since these values determine the thermodynamic feasibility of photoinduced electron transfer from the excited chlorin e6 into the TiO_2 conduction band

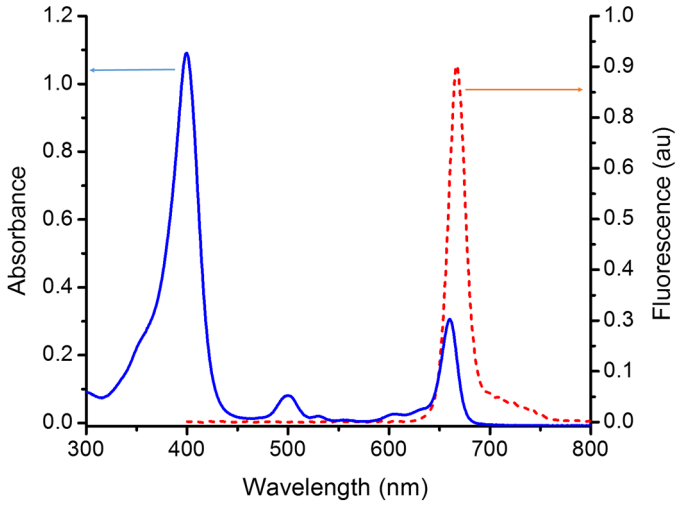

Fig. 2 Absorption (solid line) and fluorescence (dashed line) spectrum of chlorin e6 in methanol.

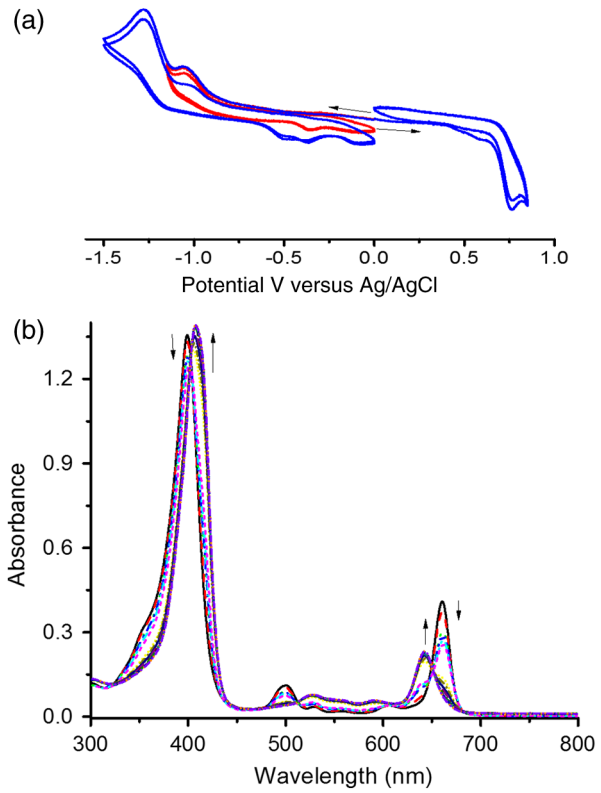

Fig. 3 (a) Cyclic voltammograms of chlorin e6 in dimethylformamide containing 0.1 M(TBA)ClO_4; scan rate = 100 mV/s. (b) Spectral changes observed during chemical oxidation of chlorin e6 using nitrosonium tetrafluoroborate (0.2 eq each addition) in methanol.

$$E^o(\mathrm{Ce6}^+/{}^1\mathrm{Ce6}^*) \sim E^o(\mathrm{Ce6}^+/\mathrm{Ce6}) - E_{0-0}/e, \tag{1}$$

$$\Delta G_{\mathrm{inj}} = E^o(\mathrm{Ce6}^+/{}^1\mathrm{Ce6}^*) - E_{\mathrm{CB}}(\mathrm{TiO_2}), \tag{2}$$

where $E^o(\mathrm{Ce6}^+/{}^1\mathrm{Ce6}^*)$ is the excited-state potential for the chlorin e6 radical cation/singlet excited chlorin e6 couple, $E^o(\mathrm{Ce6}^+/\mathrm{Ce6})$ is the ground-state potential for the chlorin e6 radical cation/chlorin e6 couple, E_{0-0} is the estimated chlorin e6 ground state to chlorin e6 singlet-state transition energy ($S_0 - S_1$ energy difference, 1.87 eV), and e is the elementary charge of an electron. ΔG_{inj} is the free-energy change for electron injection and E_{CB} is the conduction band edge potential of TiO_2 (−0.57 V versus NHE). Such calculations resulted in a $E^o(\mathrm{Ce6}^+/{}^1\mathrm{Ce6}^*)$ value of −1.15 eV and a ΔG_{inj} value of −0.58 eV, respectively. As seen from this data, the excited state reduction potential is more negative (higher in energy) than the conduction band edge of TiO_2; thus electron injection is possible from the S_1 state of chlorin e6 to the conduction band of TiO_2.

In order to visualize the spectral features of the oxidized electron donor, chlorin e6 was chemically oxidized by the addition of one equivalent of nitrosonium tetrafluoroborate in methanol. Figure 3(b) shows the associated spectral changes. New bands with peak maxima at 408, 526, 591, and 642 nm were observed for the $Ce6^+$ species. Transient formation of such peaks in femtosecond transient spectroscopy studies provides evidence of charge injection from Chlorin e6 (*vide infra*).

Molecular orbital calculations using B3LYP/6-31G* basis set[25,26] were performed to arrive at the geometry and electronic structure of chlorin e6. The structure was fully optimized on Born–Oppenheimer potential energy surface and the frequency calculations revealed the absence of negative frequencies. Figure 4(a) shows the optimized structure, whereas Figs. 4(b) and 4(c) show the Frontier HOMO and LUMO. In the optimized structure, the carboxy group connected directly to the β-pyrrole ring was in-plane with the macrocycle. However, the two carboxy

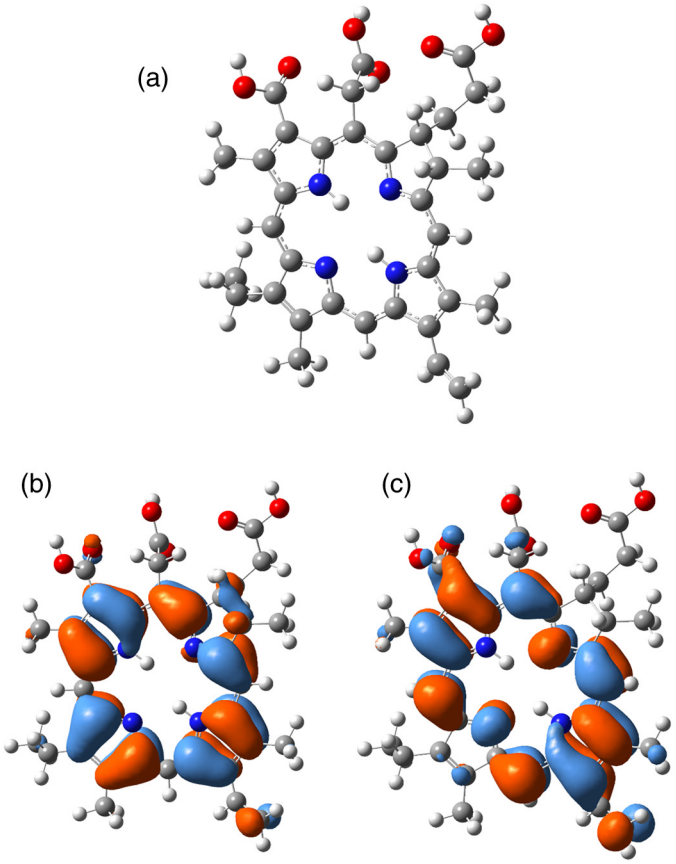

Fig. 4 (a) B3LYP/6-31G* optimized structure, (b) Frontier HOMO, and (c) Frontier LUMO of chlorin e6.

groups with alkyl linkers, viz., CH_2—COOH and CH_2—CH_2—COOH were located just above the plane of the macrocycle. The Frontier HOMO was found to be fully localized on the chlorin e6 without much contribution on the carboxyl groups. Interestingly, the LUMO was extended all the way to the carboxylic acid group that was in-plane with the macrocycle. This result suggests that the excited state charge injection would likely follow through this carboxylic acid group attached to TiO_2 surface.

3.2 *Photoelectrochemical and Impedance Spectroscopy Studies*

Figure 5(a) shows the J–V characteristics of DSSCs employing chlorin e6 as a photosensitizer under AM 1.5 solar illumination conditions. Both working and counter electrodes were sandwiched together, using the thin film TiO_2 as the working electrode, platinized FTO as the counter electrode and employing a solution containing I^-/I_3^- as the redox mediator between the electrode interfaces. The electrodes were soaked for different time intervals in 0.3 mM chlorin e6 solution. Losses due to light reflection from the surface of the electrodes have not been corrected. On–off switching experiments were performed, resulting in steady photocurrent in the reported electrodes [Fig. 5(b)]. The open-circuit potential (V_{oc}), short-circuit current (J_{sc}), fill factor (FF), and quantum efficiency (η) were calculated according to standard procedures.[27] The highest efficiency (η) obtained was 2.1% for the cell soaked for 1 h. A gradual decrease in efficiency was observed for cells with higher soaking time, likely due to dye aggregation.

The IPCE, defined as the number of electrons generated by the light in the outer circuit divided by the number of incident photons, as given by Eq. (3):[28]

$$\mathrm{IPCE}(\%) = 100 \times 1240 \times I_{\mathrm{SC}}(\mathrm{mA\,cm^{-2}})/[\lambda(\mathrm{nm}) \times P_{\mathrm{in}}(\mathrm{mW\ cm^{-2}})], \tag{3}$$

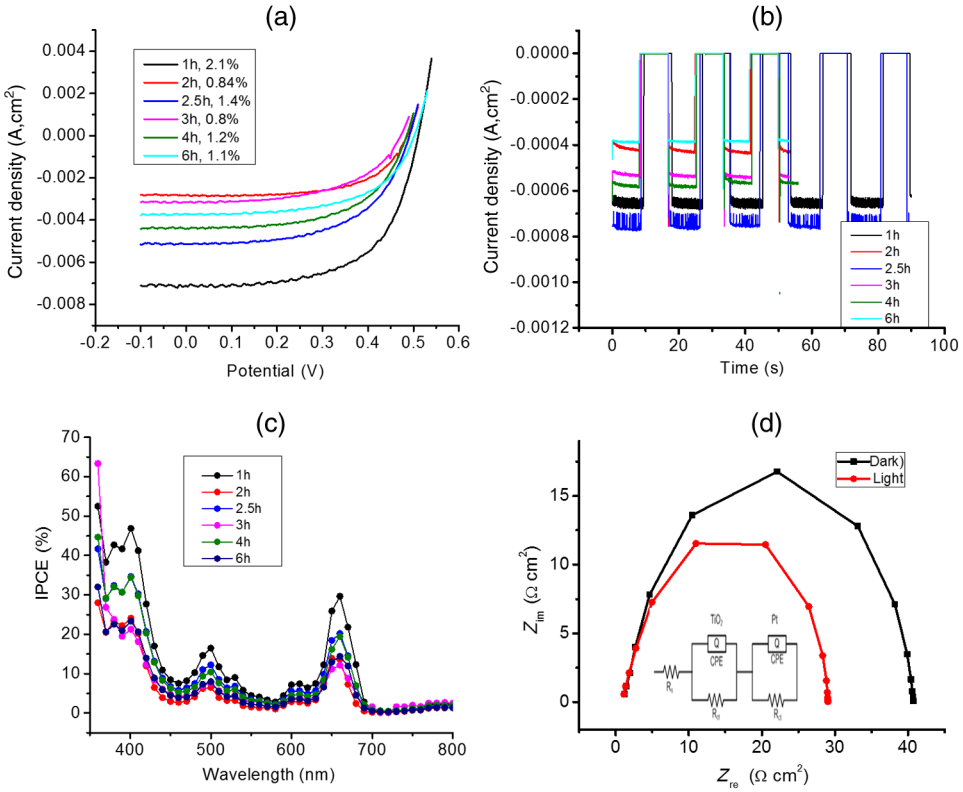

Fig. 5 (a) Photocurrent density versus voltage (J–V) curves of TiO_2/chlorin e6 DSSCs under irradiation of AM 1.5 G simulated solar light (100 mW cm^{-2}) in the presence of I^-/I_3^- redox mediator [0.6 M propyl methyl iodide (PMII), 0.1 M LiI, 0.05 M I_2, and 0.5 M tert-butylpyridine (TBP)] in acetonitrile, (b) effect on photocurrent during light on–off switching, (c) incident photon-to-current efficiency action (IPCE %) spectra for the cells shown in Fig. 4(a), and (d) Nyquist plots under dark and light conditions measured at the respective V_{oc} for the best performing TiO_2/chlorin e6 cell (figure inset = equivalent circuit diagram used to calculate charge transfer resistance).

where I_{sc} is the short-circuit current generated by incident monochromatic light illumination and λ is the wavelength of this light at an intensity of P_{in}. The IPCE spectra are shown in Fig. 5(c). Chlorin e6 generated appreciable amounts of photocurrent over the range of 350 to 700 nm.

Further, EIS studies were performed as this technique is useful for estimating electron recombination resistance and observing the dye regeneration efficiency.[29,30] The Nyquist plot for the best performing cell is shown in Fig. 5(d). The large semicircle in the low-frequency range corresponds to the TiO_2/chlorin e6/redox (I^-/I_3^-) electrolyte interface.[29,30] The curves were analyzed using an equivalent circuit [Fig. 4(d), inset]. The charge transfer resistance, R_{ct}, was found to be lower for the TiO_2/Ce6/redox interface under light illumination (26.4 Ω cm^2) compared to the value gathered in dark conditions (39.0 Ω cm^2).

In order to understand the effect of co-adsorbent on the cell performance, a two-step procedure was adapted. In the first step, various amounts of co-adsorbents (0.7 to 5.4 mM) in the presence of chlorin e6 (0.3 mM) soaked for 3 h were used to establish the optimum concentration of co-adsorbent. In the second step, the optimum concentration of co-adsorbent from step 1 and chlorin e6 was allowed for different soaking times to obtain the optimum soaking time for best cell performance.

Figure 6 summarizes results of solar cells using deoxycholic acid as a co-adsorbent. Under the experimental conditions, the optimum concentration of co-adsorbent was 0.7 mM [Fig. 6(a)] which resulted in a 1.6% solar cell efficiency. Next, using 0.3 mM chlorin e6 and 0.7 mM deoxycholic acid, cells of varying soaking times were recorded. As shown in Fig. 6(b), the best cell performance was for the cell that was soaked for 2 h (3.18% efficiency). The corresponding IPCE (%) curves are shown in Fig. 6(c), better photon-to-current conversion throughout the visible region (350 to 700 nm) was noted. The calculated R_{ct} values from impedance spectroscopy

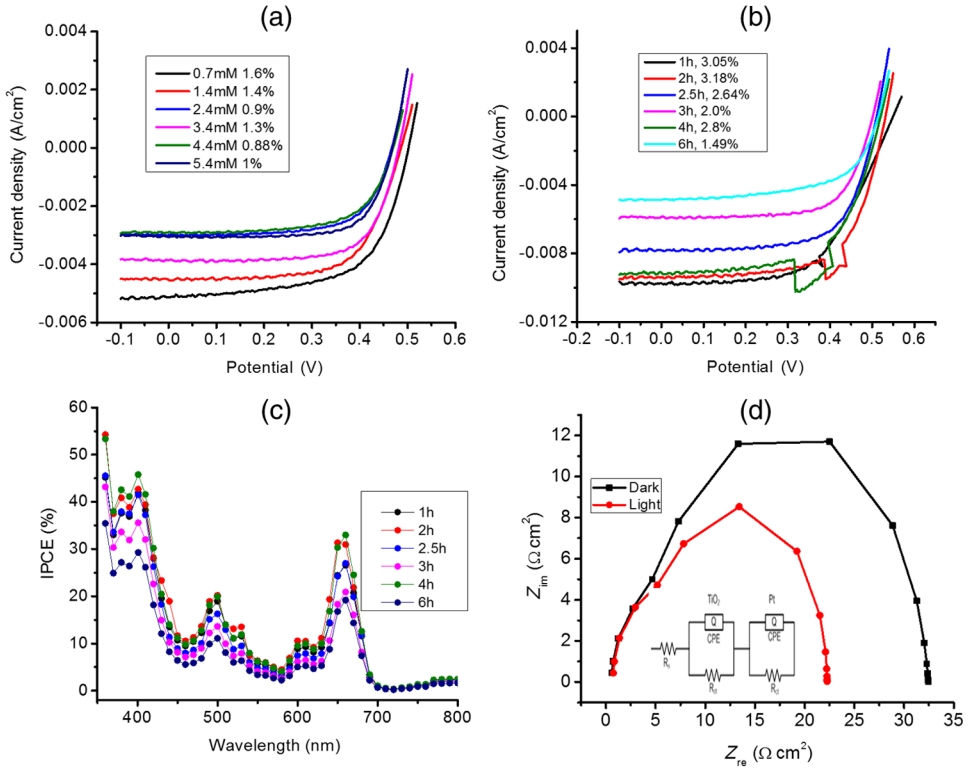

Fig. 6 (a) Photocurrent density versus voltage (J–V) curves of TiO_2/chlorin e6 in the presence of various amounts of deoxycholic acid cells under irradiation of AM 1.5 G simulated solar light (100 mW cm^{-2}) in the presence of I^-/I_3^- redox mediator (0.6 M PMII, 0.1 M LiI, 0.05 M I_2, and 0.5 M TBP) in acetonitrile, (b) J–V curves of TiO_2/chlorin e6 in the presence 0.7 mM deoxycholic acid cells at different soaking times, (c) IPCE % spectra for the cells shown in Fig. 5(b), and (d) Nyquist plots under dark and light conditions measured at the respective V_{oc} for the best performing TiO_2/chlorin e6+deoxycholic acid cell (figure inset = equivalent circuit diagram used to calculate charge transfer resistance). The bump in 2- and 4-h I–V traces is an experimental artifact.

[Fig. 6(d)] under dark and light conditions were found to be 15.4 and 8.4 Ω cm^2, respectively.

Figure 7 shows results obtained for TiO_2/chlorin e6 cells with cholic acid as co-adsorbent. The best cell performance with respect to cholic acid concentration was for the cell having 2.4 mM cholic acid [Fig. 7(a)]. Using this concentration of co-adsorbent and different soaking times, the best performance of 2.42% was achieved for the cell with 3 h soaking time [Fig. 7(b)]. The IPCE (%) shown in Fig. 7(c) shows this effect of improved light-to-current conversion efficiency in the visible region of the spectrum. The calculated R_{ct} values from the impedance spectroscopy [Fig. 7(d)] under dark and light conditions were found to be 31.6 and 18.6 Ω cm^2, respectively. It is important to note that R_{ct} value under light illumination conditions was much lower for the cells having co-adsorbents compared to the cell without co-adsorbent. Decreased R_{ct} under illumination indicates an increase in the electron injection into TiO_2/electrolyte interface layer from chlorin e6 due to decreased aggregation effects. This understanding should reflect in the transient measurements of electron injection and recombination dynamics.

3.3 *Femtosecond Transient Absorption Spectral Studies*

In order to rationalize the observed better performance of the cells in the presence of co-adsorbents, the charge injection and recombination dynamics were studied for FTO/TiO_2/chlorin e6 with and without co-adsorbents. The amount of co-adsorbent and soaking time for a given cell assembly was taken from the study described in the previous section.

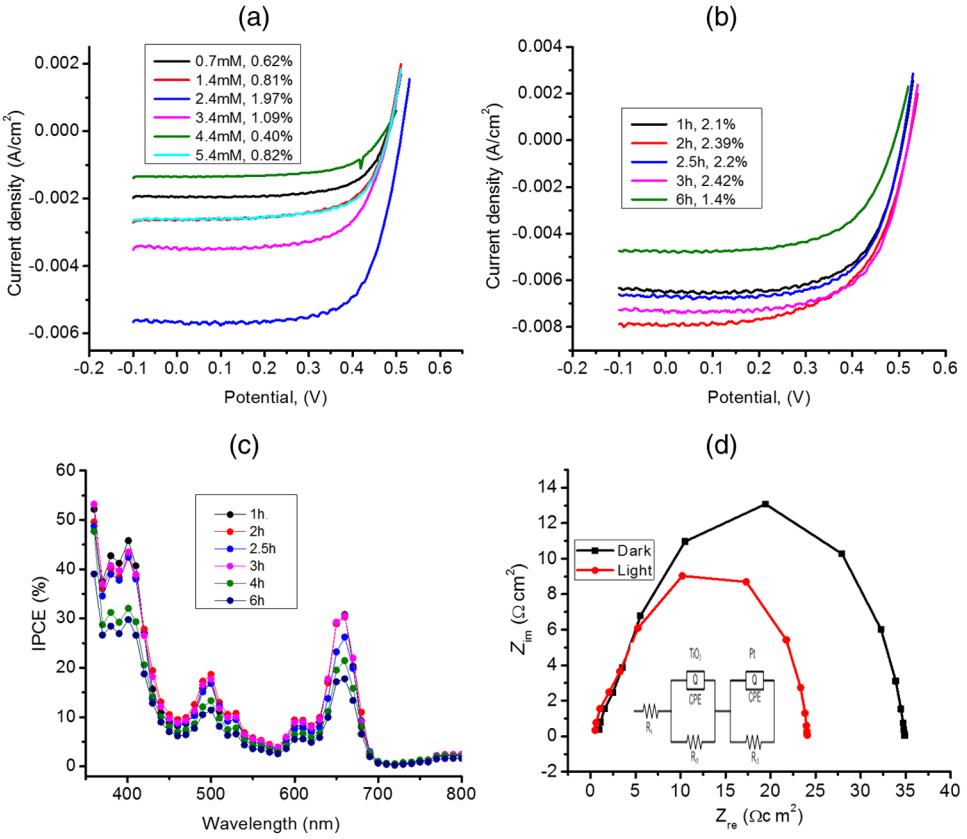

Fig. 7 (a) Photocurrent density versus voltage (J–V) curves of TiO_2/chlorin e6 in the presence of various amounts of cholic acid cells under irradiation of AM 1.5 G simulated solar light (100 mW cm^{-2}) in the presence of I^-/I_3^- redox mediator (0.6 M PMII, 0.1 M LiI, 0.05 M I_2, and 0.5 M TBP) in acetonitrile, (b) J–V curves of TiO_2/chlorin e6 in the presence 2.4 mM deoxycholic acid cells at different soaking times, (c) IPCE % spectra for the cells shown in Fig. 6(b), and (d) Nyquist plots under dark and light conditions measured at the respective V_{oc} for the best performing TiO_2/chlorin e6+cholic acid cell (figure inset = equivalent circuit diagram used to calculate charge transfer resistance).

Figure 8(a) shows the femtosecond transient spectra of chlorin e6 in methanol at the indicated delay times. Singlet excited state features were immediately observed upon excitation. Positive peaks at 482, 518, 542, 572, and 620 nm and bleached peaks at 500, 530, 608, and 670 nm were observed. Except for the 670-nm peak, all these peaks correspond to ground-state depletion. The 670-nm peak has contributions from both ground-state depletion and stimulated emission of chlorin e6. The time profile of the 670-nm peak shows slow recovery which is consistent with the relatively long lifetime of chlorin e6 (4.73 ns).

Figure 8(b) shows transient spectra at the indicated time intervals of FTO/TiO_2/chlorin e6 electrode. As expected for chlorin e6$^+$ from Fig. 3(b), strong peak at 582 nm, that was absent for pristine chlorin e6 was observed providing evidence for charge injection from the singlet excited state of chlorin e6 to the conduction band of TiO_2, an observation similar to that reported earlier for FTO/TiO_2/porphyrin and phthalocyanine-based solar cells.[23,31,32] The time profile of this peak could be fitted satisfactorily to a biexponential decay fit resulting in time constants of 0.88 and 24.7 ps. The rate of charge injection, k_{CI}, and charge recombination, k_{CR}, evaluated from these time constants were found to be 1.14×10^{12} and 4.05×10^{10} s^{-1}, respectively. The magnitude of these values was close to that reported for porphyrin-based solar cells.[23,31–33]

Figures 8(c) and 8(d) show transient spectra of FTO/TiO_2/chlorin e6+cholic acid and FTO/TiO_2/chlorin e6+deoxycholic acid electrodes. The spectral features were quite similar to that gathered for the FTO/TiO_2/chlorin e6 electrode suggesting that the co-adsorbent does not directly interact with the sensitizer to change the spectral features. By monitoring the time

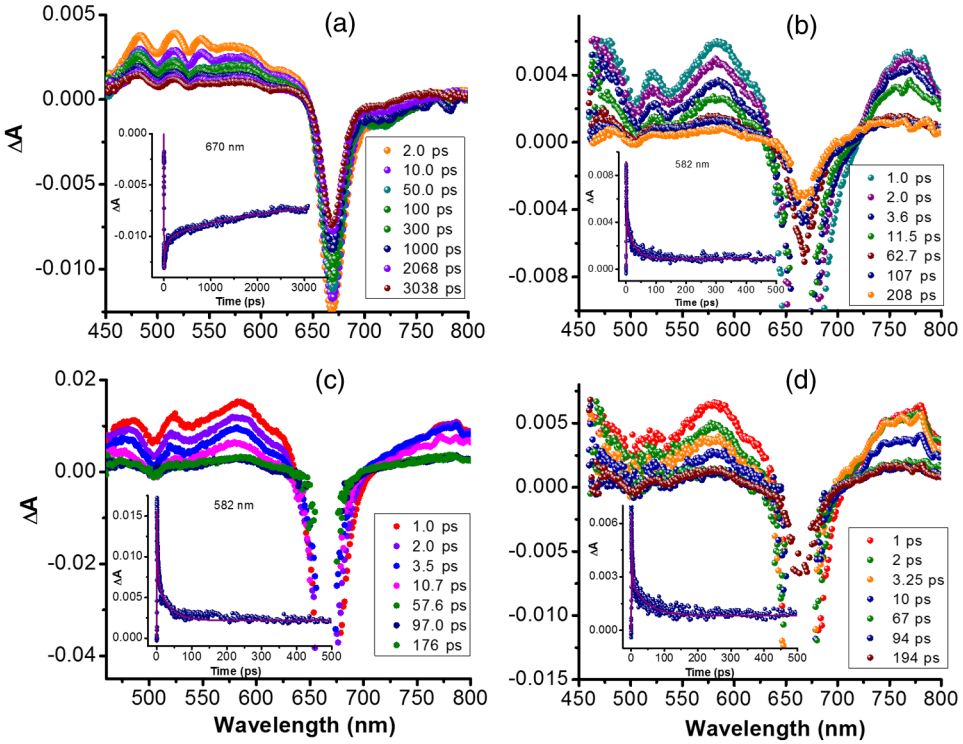

Fig. 8 Femtosecond transient absorption spectra of (a) chlorin e6 in methanol at the indicated delay times (inset: time profile of the 670-nm peak), (b) FTO/TiO_2/chlorin e6 electrode (inset: time profile of the 582-nm peak), (c) FTO/TiO_2/chlorin e6+cholic acid (inset: time profile of the 582-nm peak), and (d) FTO/TiO_2/chlorin e6+deoxycholic acid electrode (inset: time profile of the 582-nm peak). The samples were excited using 400 nm laser pulses of 100 fs.

profile of the 582-nm peak of chlorin e6+, the rise and decay time constants, and the k_{CI} and k_{CR} values were evaluated from the biexponential decay fit. For the FTO/TiO_2/chlorin e6+cholic acid electrode, the time constants were found to be 2.54 and 34.1 ps, resulting into k_{CI} and k_{CR} values of 4.0×10^{11} and 3.0×10^{10} s^{-1}, respectively. For the FTO/TiO_2/chlorin e6+deoxycholic acid electrode, the time constants were found to be 2.3 and 48.3 ps, resulting into k_{CI} and k_{CR} values of 4.35×10^{11} and 2.1×10^{10} s^{-1}, respectively. It is clear from this data that the presence of co-adsorbent influences both k_{CI} and k_{CR}, more so for k_{CR} by reducing charge recombination rate by an order of magnitude. These results along with the aforementioned reduced charge transfer resistance values from impedance spectroscopy for the electrodes having co-adsorbents provide a rational explanation for the observed improved cell performance.

4 Summary

The effect of solar cell performance improving co-adsorbents, cholic acid and deoxycholic acid, is rationalized by a systematic study involving electrochemical impedance and femtosecond transient spectroscopy studies. The DSSCs were built using chlorin e6 adsorbed onto TiO_2 surface in the absence and presence of co-adsorbents. The amount of co-adsorbent and soaking time was varied for optimum cell performance by recording J–V and IPCE (%) curves. The EIS studies gave lower charge transfer resistance, which translated to better dye regeneration efficiency for co-adsorbed cells compared to the cells with no co-adsorbent. The kinetics of charge injection and charge recombination on the TiO_2/chlorin e6/adsorbent electrodes, determined from femtosecond transient absorption studies, were revealed to be slower by an order of magnitude for charge recombination rates for electrodes co-adsorbed either with cholic acid or deoxycholic acid. Better dye regeneration and slower charge recombination resulted in overall improved performance of the present chlorin e6-based DSSCs. Further studies along this line are in progress in our laboratory.

Acknowledgments

This work was supported by the National Science Foundation (Grant No. 1401188).

References

1. B. O'Regan and M. Grätzel, "A low-cost, high-efficiency solar cell based on dye-sensitized colloidal TiO_2 films," *Nature* **353**(6346), 737–740 (1991).
2. A. Yella et al., "Porphyrin-sensitized solar cells with cobalt (II/III)-based redox electrolyte exceed 12 percent efficiency," *Science* **334**(6056), 629–634 (2011).
3. Y. Ooyama and Y. Harima, "Molecular designs and syntheses of organic dyes for dye-sensitized solar cells," *Eur. J. Org. Chem.* **2009**(18), 2903–2934 (2009).
4. H. Imahori, T. Umeyama, and S. Ito, "Large π-aromatic molecules as potential sensitizers for highly efficient dye-sensitized solar cells," *Acc. Chem. Res.* **42**(11), 1809–1818 (2009).
5. X.-F. Wang and H. Tamiaki, "Cyclic tetrapyrrole based molecules for dye-sensitized solar cells," *Energy Environ. Sci.* **3**(1), 94–106 (2010).
6. M. G. Walter, A. B. Rudine, and C. C. Wamser, "Porphyrins and phthalocyanines in solar photovoltaic cells," *J. Porphyrins Phthalocyanines* **14**(09), 759–792 (2010).
7. N. Koumura et al., "Alkyl-functionalized organic dyes for efficient molecular photovoltaics," *J. Am. Chem. Soc.* **128**(44), 14256–14257 (2006).
8. X.-F. Wang et al., "Chlorophyll-a derivatives with various hydrocarbon ester groups for efficient dye-sensitized solar cells: static and ultrafast evaluations on electron injection and charge collection processes," *Langmuir* **26**(9), 6320–6327 (2010).
9. X.-F. Wang et al., "Fabrication of dye-sensitized solar cells using chlorophylls c1 and c2 and their oxidized forms and from Undaria pinnatifida (Wakame)," *Chem. Phys. Lett.* **447**(1), 79–85 (2007).
10. M. Gratzel, "Dye-sensitized solar cells," *J. Photochem. Photobiol.* **4**(2), 145–153 (2003).
11. M. K. Nazeeruddin et al., "A high molar extinction coefficient charge transfer sensitizer and its application in dye-sensitized solar cell," *J. Photochem. Photobiol. A* **185**(2), 331–337 (2007).
12. W. M. Campbell et al., "Porphyrins as light harvesters in dye-sensitized TiO_2 solar cells," *Coord. Chem. Rev.* **248**(13), 1363–1379 (2004).
13. T. Hasobe, "Supramolecular nanoarchitectures for light energy conversion," *Phys. Chem. Chem. Phys.* **12**(1), 44–57 (2010).
14. X.-F. Wang et al., "A dye-sensitized solar cell using pheophytin-carotenoid adduct: enhancement of photocurrent by electron and singlet-energy transfer and by suppression of singlet-triplet annihilation due to the presence of the carotenoid moiety," *Chem. Phys. Lett.* **439**(1), 115–120 (2007).
15. X.-F. Wang et al., "Dependence of photocurrent and conversion efficiency of titania-based solar cell on the Qy absorption and one electron-oxidation potential of pheophorbide sensitizer," *J. Phys. Chem. C* **112**(11), 4418–4426 (2008).
16. X.-F. Wang et al., "Extension of pi-conjugation length along the Qy axis of a chlorophyll a derivative for efficient dye-sensitized solar cells," *Chem. Commun.* **12**, 1523–1525 (2009).
17. X.-F. Wang et al., "Efficient dye-sensitized solar cell based on oxo-bacteriochlorin sensitizers with broadband absorption capability," *J. Phys. Chem. C* **113**(18), 7954–7961 (2009).
18. A. Kay and M. Grätzel, "Artificial photosynthesis. 1. Photosensitization of titania solar cells with chlorophyll derivatives and related natural porphyrins," *J. Phys. Chem.* **97**(23), 6272–6277 (1993).
19. Y. Amao and T. Komori, "Bio-photovoltaic conversion device using chlorine-e6 derived from chlorophyll from Spirulina adsorbed on a nanocrystalline TiO_2 film electrode," *Biosens. Bioelectron.* **19**(8), 843–847 (2004).
20. M. Ikegami et al., "Chlorin-sensitized high-efficiency photovoltaic cells that mimic spectral response of photosynthesis," *Electrochemistry* **76**(2), 140–143 (2008).
21. X.-F. Wang et al., "Molecular engineering on a chlorophyll derivative, chlorin e6, for significantly improved power conversion efficiency in dye-sensitized solar cells," *J. Power Sources* **242**, 860–864 (2013).

22. G. Calogero et al., "Absorption spectra and photovoltaic characterization of chlorophyllins as sensitizers for dye-sensitized solar cells," *Spectrochim. Acta, Part A* **132**, 477–484 (2014).
23. A. S. Hart et al., "Porphyrin-sensitized solar cells: effect of carboxyl anchor group orientation on the cell performance," *ACS Appl. Mater. Interfaces* **5**(11), 5314–5323 (2013).
24. D. Rehm and A. Weller, "Kinetics of fluorescence quenching by electron and H-atom transfer," *Isr. J. Chem.* **8**(2), 259–271 (1970).
25. M. J. Frisch et al., *Gaussian 09, Revision B.01*, Gaussian, Inc., Wallingford, Connecticut (2010).
26. A. S. Hart et al., "Phenothiazine sensitized organic solar cells: effect of dye anchor group positioning on the cell performance," *ACS Appl. Mater. Interfaces* **4**, 5813–5820 (2012).
27. K. Kalyanasundaram, Ed., *Dye-Sensitized Solar Cells*, EPFL Press, Lausanne (2010).
28. T. Hasobe et al., "Organic solar cells. Supramolecular composites of porphyrins and fullerenes organized by polypeptide structures as light harvesters," *J. Mater. Chem.* **17**(39), 4160–4170 (2007).
29. J. Bisquert and F. Fabregat-Santiago, "Impedance spectroscopy: a general introduction and application to dye sensitized solar cells," Chapter 12 in *Dye-Sensitized Solar Cells*, K. Kalyanasundaram, Ed., pp. 457–554, EPFL Press, Lausanne, Switzerland (2010).
30. N. K. Subbaiyan, E. Maligaspe, and F. D'Souza, "Near unity photon-to-electron conversion efficiency of photoelectrochemical cells built on cationic water-soluble porphyrins electrostatically decorated onto thin-film nanocrystalline SnO_2 surface," *ACS Appl. Mater. Interfaces* **3**(7), 2368–2376 (2011).
31. H. B. Gobeze, S. K. Das, and F. D'Souza, "Femtosecond transient absorption study of supramolecularly assembled metal tetrapyrrole-TiO_2 thin films," *J. Phys. Chem. C* **118**(30), 16660–16671 (2014).
32. I. Obraztsov et al., "Langmuir–Blodgett films of self-assembled (alkylether-derivatized Zn phthalocyanine)–(C_{60} imidazole adduct) dyad with controlled intermolecular distance for photoelectrochemical studies," *ACS Appl. Mater. Interfaces* **6**(11), 8688–8701 (2014).
33. C.-W. Chang et al., "Femtosecond transient absorption of zinc porphyrins with oligo(phenylethylnyl) linkers in solution and on TiO_2 films," *J. Phys. Chem. C* **113**(27), 11524–11531 (2009).

Sherard K. S. Lightbourne is currently a graduate student at the University of North Texas (UNT), Denton. His research is focused on the fabrication and characterization of solar energy harvesting devices such as dye sensitizer solar cells and thin-layer photovoltaic devices. He received a BS degree in chemistry at the Jarvis Christian College, Hawkins, Texas, prior to joining UNT in 2013.

Habtom B. Gobeze is a graduate student at the University of North Texas. He received his BSc degree in chemistry from the University of Asmara, Eritrea, in 2001. Prior to joining the graduate program, he worked as a chemistry teacher in a college and as an analyst for a pharmaceutical company. His current research interests are in the area of ultrafast spectroscopy for the study of dynamics of photoinduced energy and electron transfer processes in photosynthetic model systems in solution, thin films, and at modified electrode surfaces.

Navaneetha K. Subbaiyan is a postdoctoral fellow at the center for integrated nanotechnology at Los Alamos National Laboratory, New Mexico. He received his PhD degree from the University of North Texas in 2012, and his BTech degree in chemical and electrochemical engineering from the Central Electrochemical Research Institute, Karaikudi, India, in 2006. His research interests include the design, construction, and characterization of functional metal oxides and carbon nanomaterials for applications such as solar cells and electrocatalysis.

Francis D'Souza is a university distinguished professor in chemistry and materials science and engineering at the University of North Texas, Denton. He received his BSc/MSc degrees from the Mysore University, Mysore, India (1982 and 1984) and his PhD degree from the Indian Institute of Science, Bangalore, India, in 1992. He was a postdoctoral research associate at the University of Houston and University of Dijon, France, from 1992 to 1994. Prior to joining UNT in 2011, he was a faculty member at Wichita State University, Wichita, Kansas.